INVESTIGATIVE RADIOLOGY
Volume 30, Number 12, 738–744

Hydrogen Magnetic Resonance Spectroscopy Follow-up After Radiation Therapy of Human Brain Cancer

Unexpected Inverse Correlation Between the Changes in Tumor Choline Level and Post-Gadolinium Magnetic Resonance Imaging Contrast

PAUL E. SIJENS, PHD,* CHARLES J. VECHT, MD, PHD,† PETER C. LEVENDAG, MD, PHD,‡ PIETER VAN DIJK, MSC,* AND MATTHIJS OUDKERK, MD, PHD*

Sijens PE, Vecht CJ, Levendag PC, van Dijk P, Oudkerk M. Hydrogen magnetic resonance spectroscopy follow-up after radiation therapy of human brain cancer: Unexpected inverse correlation between the changes in tumor choline level and post-gadolinium magnetic resonance imaging contrast. Invest Radiol 1995;30:738–744.

RATIONALE AND OBJECTIVES. The anatomic and metabolic changes in human brain tumors treated by radiation therapy were compared using gadolinium-enhanced magnetic resonance imaging and hydrogen (^{1}H) magnetic resonance spectroscopy. The study was intended to assess the potential of ^{1}H magnetic resonance spectroscopy in monitoring response to therapy.

METHODS. Thirteen cases of brain cancer treated by radiation therapy were examined by ^{1}H magnetic resonance spectroscopy and gadolinium-enhanced T1-weighted magnetic resonance imaging and reexamined at 2-month intervals.

RESULTS. Follow-up after radiation therapy showed changes in post-gadolinium magnetic resonance imaging contrast that are inversely correlated with the changes in choline level ($r = -0.69$, $P < 0.00001$) and in tumor volume ($r = -0.35$, $P < 0.05$).

CONCLUSIONS. The choline loss in tumors gaining post-gadolinium magnetic resonance imaging contrast after therapy is unexpected in view of previously reported correlation between the two in untreated metastatic brain tumors. Indicated is the use of ^{1}H magnetic resonance spectroscopy to discriminate enhancing brain tumors with a high content of vital tumor cells (high choline) from tumors, combining decreased cell density with increased interstitial space (low choline).

KEY WORDS. Brain tumors; gadolinium-DTPA contrast agent; magnetic resonance imaging; magnetic resonance spectroscopy.

BRAIN TUMORS have high choline (Cho) levels and reduced N-acetylaspartate (NAA) levels compared with normal brain tissue.[1] Whereas hydrogen (^{1}H) magnetic resonance spectroscopy (MRS)-detected Cho levels generally increase with tumor size and correlates with gadolinium (Gd)-DTPA enhancement in T1-weighted magnetic resonance imaging (MRI), they cannot be used as discriminators of tumor grade, because necrotic high grade tumors have low levels of Cho.[2,3] Previous ^{1}H MRS studies indicated that the lactate (Lact) frequently detected in brain tumors is neither significantly correlated with glucose use[4] nor to the grade of malignancy.[2,5,6] We recently demonstrated the preferential presence of Lact in untreated metastatic brain tumors that are necrotic and comparatively low in Cho and creatine (Cr).[3]

The purpose of this study is to compare the anatomic and metabolic changes in human brain tumors examined for the first time by Gd-enhanced MRI as well as ^{1}H

From the Departments of *Radiology, †Neurology, and ‡Radiation Therapy, Dr. Daniel den Hoed Cancer Center, Academic Hospital Rotterdam, The Netherlands.

Reprint requests: P.E. Sijens, PhD, Department of Radiology, Dr. Daniel den Hoed Cancer Center, University Hospital Rotterdam, Groene Hilledijk, 301, P.O. Box 5201, 3008 AE Rotterdam, The Netherlands.

Received July, 26 1995, and accepted for publication, after revision, September 14, 1995.

TABLE 1. Magnetic Resonance Spectroscopy of Brain Tumors in Follow-up after Radiotherapy

Case no.	Tumor type, time of reexamination	Tumor volume (cm^3)*	MRI contrast ± SD†	MRS: SV or CSI	Tumor voxel(s) (cm^3)	Metabolites‡				
						Cho	Cr	NAA	Lact	Lipid§
1	Lung ca. meta	3.1	0.84 ± 0.19	SV	8	56	49	73	0	–
	1 m later	1.3	1.04 ± 0.06	SV	8	46	47	46	0	+
2	Mammary ca. meta	0.3	1.59 ± 0.19	SV	8	48	59	67	0	–
	3 m later	0.4	1.43 ± 0.08	SV	8	64	49	75	0	+
	5 m later	0.4	1.64 ± 0.14	SV	3.4	45	43	98	0	+
3	Mammary ca. meta	3.1	1.91 ± 0.10	SV	8	66	10	0	0	+
	2 m later	1.3	2.28 ± 0.16	SV	3.4	47	33	13	193	–
	4 m later	1.4	1.72 ± 0.22							
4	Medullablast. meta	1.3	1.18 ± 0.16	SV	3.4	42	19	60	0	+
	2 m later	2.1	1.20 ± 0.25	SV	3.4	106	50	84	94	–
	4 m later	4.2	1.16 ± 0.10							
5	Melanoma meta	0.3	—	SV	8	25	28	36	20	–
	2 m later	2.3	1.50 ± 0.41	SV	8	68	60	52	30	+
	4.5 m later	2.3	1.46 ± 0.23							
6	Pr. NH lymphoma	0.3	1.03 ± 0.07	SV	8	518	0	56	0	–
	5 m later	0.0	0.81 ± 0.03¶	SV	8	43	80	73	0	–
	8 m later	0.0	0.72 ± 0.06¶							
7	Astrocytoma III	7.7	1.58 ± 0.40	SV	8	34	22	36	0	+
	2 m later	12.3	1.51 ± 0.28	SV	8	19	17	24	0	+
	4 m later	18	1.05 ± 0.22	SV	8	66	79	0	0	+
8	Astrocytoma III	15	0.80 ± 0.36	SV	8	0	0	25	134	+
	5 m later	7.8	0.75 ± 0.35							
	12 m later	29.5	1.52 ± 0.40	CSI	10.2	51	25	22	0	–
9	Astrocytoma IV	2.2	1.52 ± 0.30	SV	27	54	48	66	12	–
	4 m later	2.7	0.94 ± 0.17	SV	27	79	62	52	0	+
	6.5 m later	1.8	1.46 ± 0.44	SV	27	48	51	51	15	–
	9 m later	24.5	1.23 ± 0.29	SV	64	72	73	70	0	++
10	Astrocytoma IV	6.4	0.70 ± 0.25	SV	8	67	52	50	0	+
	3 m later	12	1.19 ± 0.17	SV	8	59	37	55	0	+
	7 m later	30	0.96 ± 0.23	SV	8	44	91	52	20	+
	11 m later	32	1.01 ± 0.30	SV	8	47	38	18	32	–
11	Astrocytoma IV	170	1.13 ± 0.43	CSI	13.6	28	22	10	26	–
	1 m later	170	—	CSI	13.6	69	12	17	60	–
	3 m later	125	0.98 ± 0.46							
12	Glioblastoma mult.	56	1.24 ± 0.45	SV	43	18	26	29	0	++
	3 m later	62	1.11 ± 0.32	SV	43	36	28	34	0	++
	5 m later	64	1.10 ± 0.55	SV	8	57	10	22	46	–
	8 m later	61	1.34 ± 0.68	SV	8	31	20	26	50	–
	11 m later	52	1.65 ± 0.46	SV	8	28	12	38	83	–
13	Glioblastoma mult.	75	1.11 ± 0.31	SV	27	39	69	0	0	++
	3 m later	92	1.26 ± 0.31	SV	27	76	66	30	0	++

* Estimated from MRI.
† Postcontrast lesion signal (at largest MRI cross section) in percent of the T1-weighted MRI signal of contralateral brain tissue.
‡ In percent of NAA in contralateral brain tissue.
§ Absent (–), low (+), high (++).
¶ At location of tumor in first examination.
MRI: magnetic resonance imaging; MRS: magnetic resonance spectroscopy; SV: single voxel; CSI: chemical shift imaging; Cho: choline; Cr: creatine; NAA: N-acetyl-aspartate; Lact: lactate; ca: carcinoma; mult: multiform; pr: primary; NH = non-Hodgkin.

MRS shortly after radiation therapy and reexamined at 2-month intervals thereafter. The presented results of ^1H MRS follow-up of brain tumors treated by radiation therapy are, to our knowledge, the first that establish correlation between changes in tumor metabolite level and post-Gd MRI contrast (pGdC).

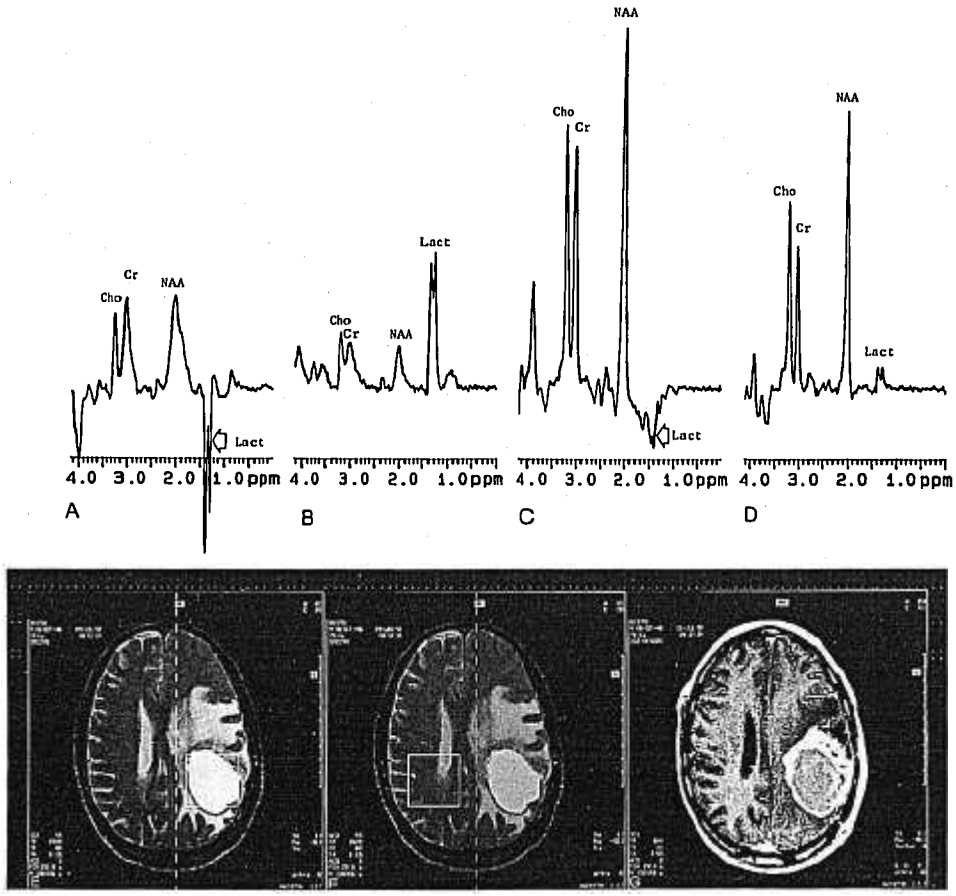

Figures 1A–1G. Single voxel ^{1}H magnetic resonance (MR) spectra of primary brain tumor (astrocytoma grade 2; A,B) and of contralateral brain tissue (C,D) measured with echo times of 135 msec (A,C) and 270 msec (B,D). T2-weighted MR images show the locations of 64-cm^3 MR spectroscopy voxels centered on tumor (E) and contralateral tissue (F). Also shown is the post-gadolinium T1-weighted MR image of an axial slice through the same region (G).

Materials and Methods

Thirteen cases of human brain cancer were examined by ^{1}H MRS and Gd-enhanced T1-weighted MRI shortly after treatment by radiation therapy (typically 1 month after external radiation therapy and/or brachytherapy) and reexamined by both MRS and MRI at intervals of 2 months (Table 1). No surgery was performed in the periods between subsequent MRS examinations. Magnetic resonance spectroscopy examinations and contrast-enhanced MRI were performed at 1.5 T using a 1.5/2 T SP63/84 Helicon whole body MR scanner (Siemens AG, Erlangen, Germany). The standard circular polarized transmit/receive head coil and 10 mT/m gradient system were used for both MRI and MRS.

The MR follow-up scheme was designed to explore possible correlation of changes in MRI and MRS parameters with simultaneous changes in tumor size. The potential of MRS for prediction or early assessment of response to radiation therapy is not featured in this study. For that purpose, a different scheme, including pretreatment examinations as well as reexaminations at multiple times after initiation of the irradiation series, would have been needed. At some of the times listed in Table 1, the MRI examinations could not, for either technical or logistic reasons, be followed by MRS. Beyond the time frame listed in Table 1, most patients received additional treatment, such as chemotherapy or surgery. Therefore, it was deemed better not to diminish the clarity of the study by providing additional clinical follow-up data.

Gadolinium-DTPA-Enhanced Magnetic Resonance Imaging

The MRI studies, preceding the MRS by up to 2 weeks, included a T1-weighted sequence (repetition time [TR]/echo time [TE], 610/14; 2 NEX; matrix size, 192 × 256; 3/4 rectangular field of view) with 6-mm slices. T1-weighted MRI was repeated 5 minutes after contrast (0.2 mmol/kg Gd-DTPA). Routines provided by the manufacturer of the MR system were used to determine the mean signal intensities and standard deviations for the largest transverse 6-mm thickness MRI cross-section of each lesion. The volume of each metastasis was estimated from the enhancing areas on postcontrast MRI. Enhancement is defined as percent difference between mean signals in largest postcontrast MRI cross-section of the tumor and contralateral brain tissue.

Single Voxel ^{1}H Magnetic Resonance Spectroscopy and Chemical Shift Imaging

Single voxel ^{1}H MRS was performed as described elsewhere.[3] Briefly, the double spin echo (DSE) sequence

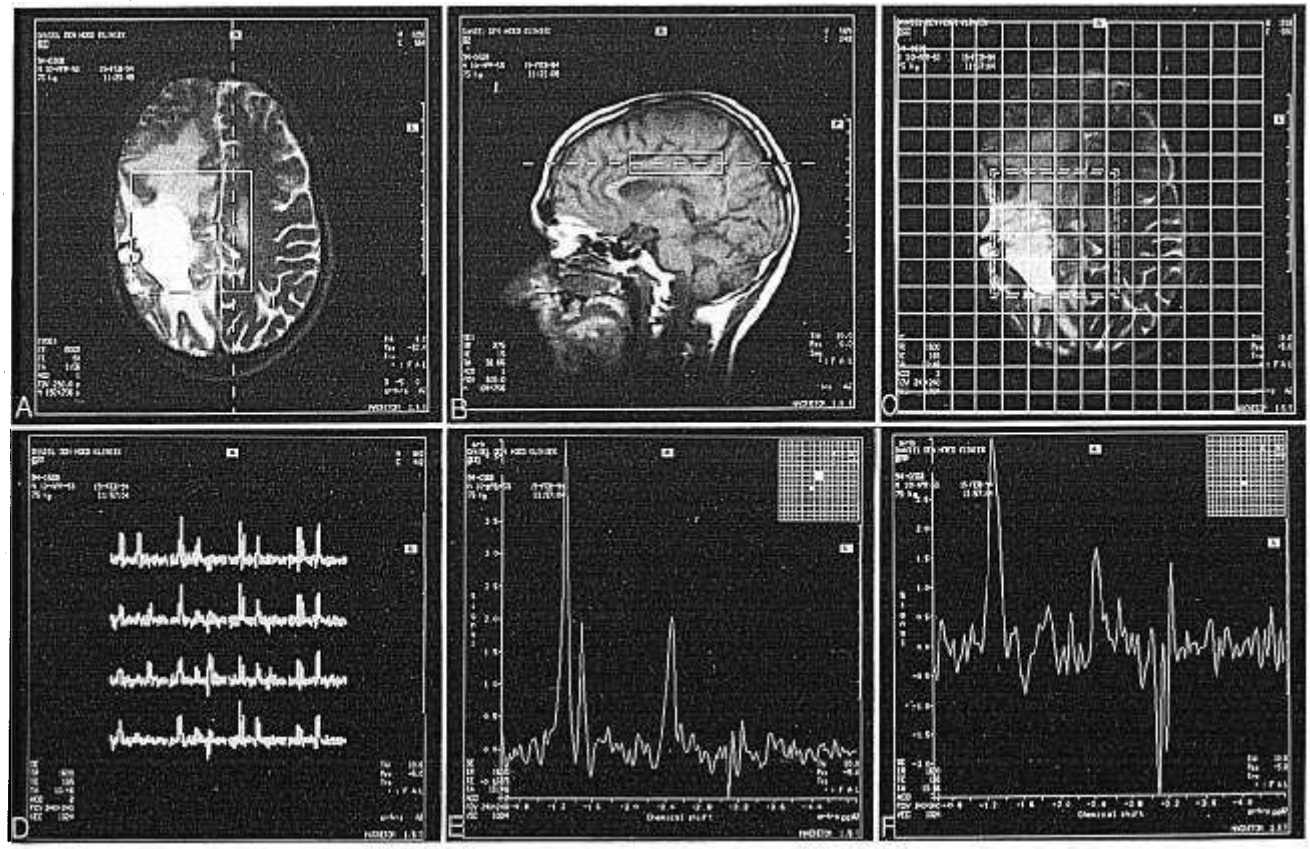

Figures 2A–2F. Hydrogen chemical shift imaging (CSI) of primary brain tumor (case 11): T2- and T1-weighted magnetic resonance images showing (A,B) volume of interest of 7·7·1.5 cm, (C,D) CSI matrix and (magnified) spectral map, and spectra of tumor voxels with elevated (E) Cho and (F) Lact.

was used to select a volume of interest in a single experimental step with suppression of the unwanted water signal.[7] Care was taken to ensure proper positioning of lesion MRS voxels in those regions that had shown signal enhancement in the Gd-DTPA-enhanced MRI studies. Magnetic resonance spectra were acquired with TE-135 msec when, because of J modulation, the doublet signal of Lact is inverted (180° out of phase) relative to the lipid signals and to the singlets of Cho, Cr, and NAA.[8] This is illustrated in Figure 1. Note the presence of a small quantity of Lact in the contralateral spectrum, probably leaked from the tumor into the cerebrospinal fluid or possibly from spatial contamination of the control voxel by tumor invasion. The whole procedure includes sagittal and transverse MRI, global shimming, volume selection, local shimming, water suppression optimization, and tumor and contralateral voxel measurements. The field homogeneity achieved in global and local shimming resulted in water peak line widths of, at most, 17 Hz and 6 Hz, respectively. With regard to the latter value, it must be realized that tumors are generally heterogeneous compared with normal brain tissue, resulting in comparative B_1-field heterogeneity and water line widths of 4 to 6 Hz, compared with 3 to 4 Hz in normal brain tissue (2 Hz in edema). DSE MR spectra were collected with 2.56-msec sinc-shaped radio frequency pulses preceded by 25.6-msec Gaussian-shaped radio frequency pulses for chemical shift selective excitation and subsequent spoiling of the resultant water signal. The second half of the spin echo was collected using 1024 data points and a spectral width of 500 Hz. All DSE measurements were the sum of 256 acquisitions with 4 prescans and TR = 1600 msec (acquisition time, 6.57 minutes). Typically, time domain data were 0 filled to 4096 points, multiplied with a Gaussian function (center, 0 msec; half-width, 256 msec), Fournier-transformed, phase-corrected, and fitted to Lorentzian curves. Quantitative analysis of patient spectra was confined to Cho (chemical shift, 3.21 ppm), Cr (3.02 ppm), NAA (2.01 ppm), and Lact (doublet centered at 1.32 ppm with coupling constant of 7 Hz). In accordance with previous work,[3] Cho, Cr, and Lact are presented in percent of the NAA detected in contralat-

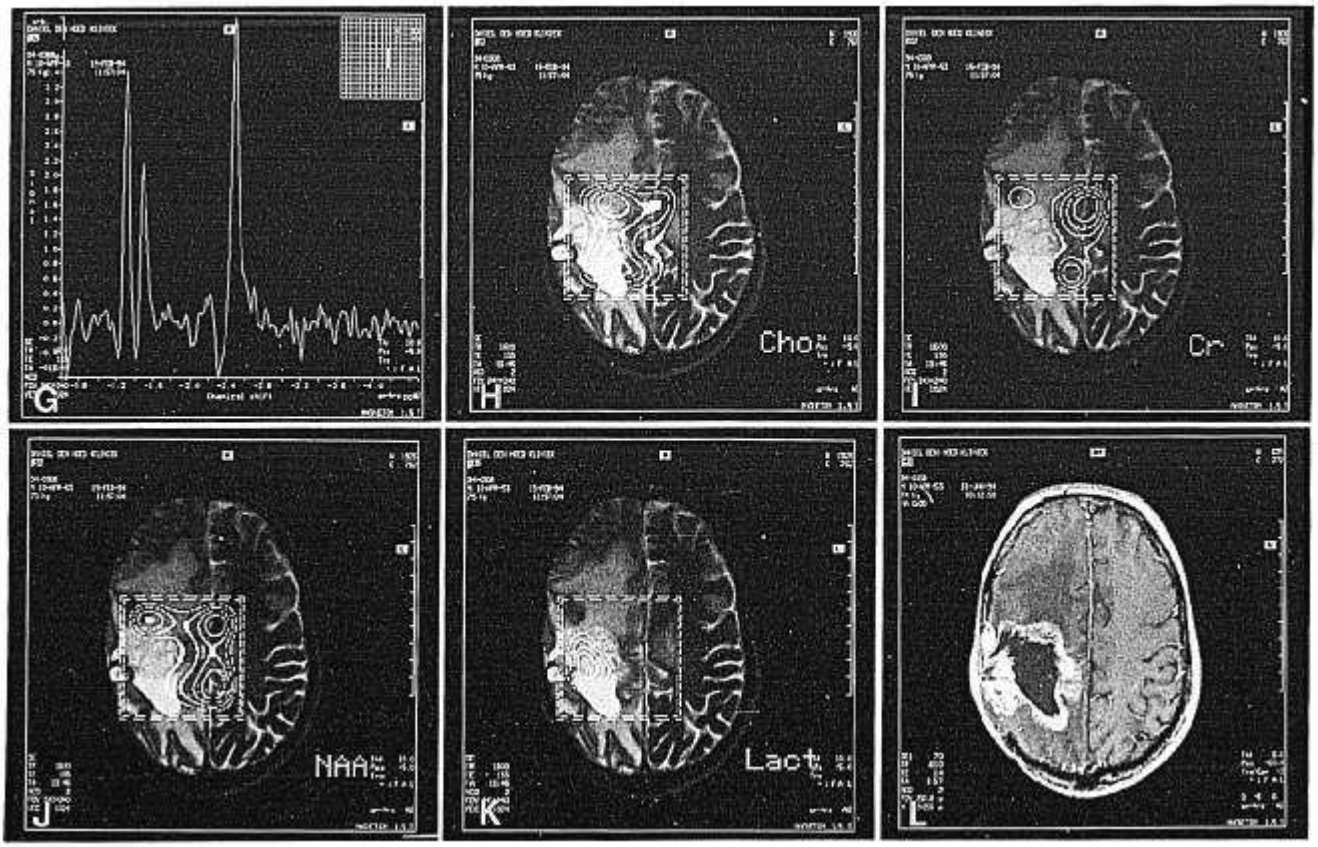

Figures 2G–2L. Magnetic resonance spectrum of normal brain tissue included in the volume of interest (G) and metabolic maps showing the distributions of (H) Cho, (I) Cr, (J) NAA, and (K) Lact. Chemical shift imaging voxel size: 3.4 cm^3; echo time 135 = msec. Also shown is the post-gadolinium T1-weighted magnetic resonance image of an axial slice through the same region (L).

eral brain tissue and not corrected for saturation and relaxation effects. Lipid peak areas (0.9 ppm and 1.3 ppm) were not quantitated because in peripheral voxels signal contributions from subcutaneous fat and bone marrow were often significant.

A hybrid chemical shift imaging (CSI) technique was used with two-dimensional (2D) phase encoding of a transverse slice, up to 10 · 10 · 1.5 cm^3 depending on the location of the tumor in the brain, selected with field gradients of 0.8, 0.8, and 3.0 mT/m, respectively. The CSI measurements were preceded by MRI, global shimming, and local shimming on the whole volume of interest using a single voxel DSE sequence as described in the previous paragraph. The field homogeneity achieved in global and local shimming resulted in water peak line widths of at most 17 Hz and 8 Hz, respectively. Hybrid DSE 2D CSI was subsequently applied on the 1.5-cm thickness transverse slice centered on the tumor, yielding voxels of 1.5 · 1.5 · 1.5 cm^3. Spectral maps (16 × 16 matrix defined by phase encoding, field of view 24 · 24 cm) were collected with 2.56-msec sinc-shaped radio frequency pulses preceded by 25.6-msec Gaussian-shaped radio frequency pulses for chemical shift selective excitation and subsequent spoiling of the resultant water signal. The second half of the spin echo was collected using 1024 data points and a spectral width of 500 Hz. All hybrid DSE 2D CSI measurements were the sum of two acquisitions with four prescans and TR = 1600 msec (acquisition time, 13 minutes). After retrospective positioning of voxels on tumor, time domain data were multiplied with a Gaussian function (center, 0 msec; half-width, 256 msec), 2D Fournier-transformed, phase-corrected, and quantitated as the single voxel MRS data. The whole procedure, including sagittal and transverse MRI, global shimming, volume selection, local shimming, water suppression optimization, and the measurement of one 2D spectral map, took 50 minutes.

Statistics

Correlation analyses were applied and two-tailed Student's *t* test was used in assessing the significance of the presented linear correlations.

Results

The result of CSI examination of a large brain tumor is presented in Figure 2 (case 11). The transverse cross-section of the 170 cm^3 R-parietal astrocytoma shows reduced Cr and NAA levels and high Cho levels in tumor. Lactate is localized in the necrotic center of the ring-enhancing lesion, and significant lipid signals are not detected. The peak integrals of Cho, Cr, NAA, and Lact in 4 tumor voxels, combined relative to the NAA level in the normal brain tissue included in the volume of interest, are listed in Table 1 along with the results in another 12 cases (mostly smaller tumors examined by single voxel MRS).

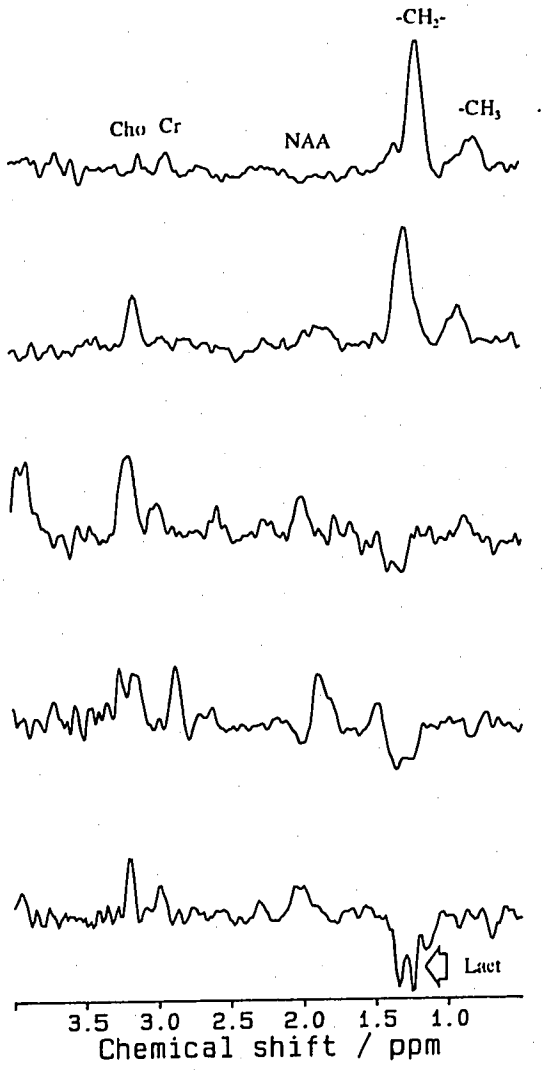

Figure 3. Single voxel ^1H magnetic resonance spectra of the same central region of irradiated glioblastoma multiform examined five times at intervals of 2 to 3 months (case 12; voxel size: 8 cm^3, echo time 135 = msec). Total tumor volume, 56 cm^3 shortly after radiation therapy (top spectrum), increased to a maximum of 64 cm^3 (middle), followed by a decrease to 52 cm^3 (bottom).

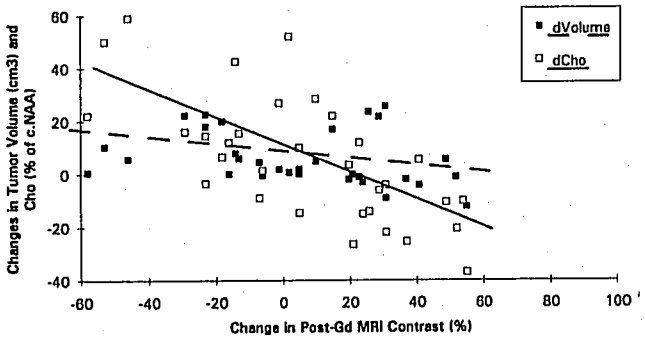

Figure 4. Changes in lesion Cho level, corrected for normal tissue contributions, and tumor volume plotted against the change in post-gadolinium magnetic resonance imaging contrast for tumors examined multiple times. Linear regression analysis: $r = -0.69$ and $P < 0.00001$ (lesion Cho), and $r = -0.35$ and $P < 0.05$ (tumor volume).

Hydrogen MRS follow-up of patients was initiated shortly after irradiation of metastatic (cases 1 to 5) and primary brain tumors (cases 6 to 13). The results are diverse. Changes in tumor Cho, Cr, and Lact signals are not correlated with changes in tumor volume ($P > 0.2$). Figure 3 shows the results for a primary brain tumor, examined five times during the first year after radiation therapy (case 12). Initial increases in tumor Cho signal during tumor progression and subsequent disappearance of the intense CH_2 and CH_1 lipid signals (compare the first three spectra from top) are followed by the appearance of an increasingly intense Lact signal and Cho decrease during tumor shrinkage. On Gd-enhanced MRI, the tumor remains highly heterogeneous, whereas pGdC decreases with initial tumor progression and increases with subsequent tumor regression (Table 1). The decreases in the intensities of lipid signals and the appearance of Lact were more or less general phenomena because these were also observed in cases 3, 4, 9, and 10 (see Discussion). The main finding in this study is that in the 13 follow-up cases combined, the changes in pGdC are inversely correlated to the changes in lesion Cho level; that is, Cho level corrected for normal tissue contributions as described elsewhere[3]: lesion Cho = Cho − ½NAA, ($r = -0.69$, $P < 0.00001$; $n = 32$) and in tumor volume ($r = -0.35$, $P < 0.05$) (Fig. 4). Additional correlations between changes in MRS-determined metabolite levels and MRI-determined tumor volume, pGdC, and heterogeneity do not reach significance.

Discussion

The initial ^1H MR spectra of metastatic (cases 1 to 5) and primary brain tumors (cases 6, 7, and 9 to 13) mea-

sured shortly after termination of radiation therapy, although quite divergent, share a reduced NAA/Cho ratio compared with contralateral brain tissue (0.91 ± 0.18 SEM versus 1.94 ± 0.06 [corpus nuclei caudati] to 2.68 ± 0.05 [lobus occipitalis] in normal brain tissue). This feature, observed in 12 out of 13 cases, is in line with the observations in untreated primary[2,9,10] and metastatic brain tumors.[3,11] Remarkable is the abnormality of the MR spectra of volumes containing only 4% MRI-visible metastatic tumor (cases 2, 5, and 6). This might be interpreted as evidence that early stage brain metastases are only partially visualized with Gd-enhanced MRI. Tumor Cho levels higher than those in contralateral brain tissue were observed in only five patients (cases 1, 3, 6, 9, and 10). Creatine levels varied considerably between tumors (0.31 ± 0.06 SEM). Evaluation of data in terms of relative concentrations or in the tumor metabolite ratios of NAA per Cr and Cr per Cho did not yield significant, additional information compared with expression in percent of contralateral NAA (see Materials and Methods). The Lipid signals were observed in seven cases and Lact in only four cases. Comparison of the findings in cases 2 and 3 (mammary carcinoma metastasis), 7 and 8 (astrocytoma III), and 12 and 13 (glioblastoma multiforme) indicates that the presence or appearance of Lact signal does not depend on tumor type, in agreement with a previous report.[12]

The presented results of brain tumor follow-up are, to our knowledge, the first that establish correlation between changes in the levels of a tumor metabolite and changes in pGdC. The Cho loss in tumors gaining pGdC after therapy is unexpected in view of previously reported positive correlation between Cho and Gd enhancement in untreated metastatic brain tumor.[3] It is concluded that in irradiated (and probably also in otherwise treated) brain tumors, there is no predictable relationship between the appearance of Gd-enhanced MRI and the results of ^{1}H MRS. This result, the absence of correlation between the results of the imaging method most frequently used to detect and monitor brain tumors and MRS findings, implies a diagnostic application: ^{1}H MRS can be used to discriminate Gd-enhancing brain tumor with a high content of vital tumor cells (high Cho) from similarly enhancing tumor that, typically after cell kill, combines decreased cell density with increased interstitial space (low Cho).

In five cases, there were decreases in lipid signal that were followed by increases in Lact. In case 9, there was less consistency with alternating rises and falls in both tumor metabolite levels (Cho, lipids, Lact) and in tumor volume. The lipid signals, while influenced by signal contributions from subcutaneous fat and bone marrow, may essentially reflect mobile lipid accumulation in necrotic foci below MRI resolution, as has been reported for high-grade astrocytomas examined in vitro.[9] The lipid decreases with appearance of Lact in the tumor MR spectra could thus be explained by the replacement of microscopic necrosis by MRI visible areas of gross necrosis,[3] as observed with tumor progression (case 10) and therapy-induced regression (case 12).

Acknowledgments

The authors thank Deni J.A. Kraus for participating in the data acquisition and Dr. Rolf Sauter (Siemens AG, Erlangen, Germany) for providing works-in-progress CSI sequences.

References

1. Negendank W. Studies of human tumors by MRS: A review. NMR Biomed 1992;5:303–324.
2. Fulham MJ, Bizzi A, Dietz MJ, et al. Mapping of brain tumor metabolites with proton MR spectroscopic imaging: Clinical relevance. Radiology 1992;185:675–686.
3. PE Sijens, van Dijk P, Oudkerk M. Correlation between choline level and Gd-DTPA enhancement in patients with brain metastases of mammary carcinoma. Magn Reson Med 1994;32:549–555.
4. Alger JR, Frank JA, Bizzi A, et al. Metabolism of human gliomas: Assessment with H-1 MR spectroscopy and F-18 fluorodeoxyglucose PET. Radiology 1990;177:633–641.
5. Demaerel P, Johannik K, Van Hecke P, et al. Localized ^{1}H NMR spectroscopy in fifty cases of newly diagnosed intracranial tumors. J Comput Assist Tomogr 1991;15:67–76.
6. Kugel H, Heindel W, Ernestus RI, Bunke J, du Mesnil R, Friedmann G. Human brain tumors: Spectral patterns detected with localized H-1 MR spectroscopy. Radiology 1992;183:701–709.
7. Hentschel D, Ladebeck R. Quantitative in vivo ^{1}H MR spectroscopy of healthy and tumorous human brain tissue at 4 Tesla. Appl Magn Reson 1990;1:379–412.
8. Sotak CH, Freeman DM. A method for volume-localized lactate editing using zero-quantum coherence created in a stimulated-echo pulse sequence. J Magn Reson 1988;77:382–388.
9. Gill SS, Thomas DGT, Van Bruggen N, et al. Proton MR spectroscopy of intracranial tumors: In vivo and in vitro studies. J Comput Assist Tomogr 1990;4:497–504.
10. Negendank W, Zimmerman R, Gotsis E, et al. A cooperative group study of ^{1}H MRS of primary brain tumors. In: Proc SMRM, 12th Annual Meeting. Berkeley, CA: Society of Magnetic Resonance in Medicine, 1993;1521.
11. Sijens PE, Knopp MV, Brunetti A, et al. ^{1}H MR spectroscopy in patients with metastatic brain tumors: A multi-center study. Magn Reson Med 1995;33:818–826.
12. Kuesel AC, Sutherland GR, Halliday W, Smith ICP. ^{1}H MRS of high grade astrocytomas: Mobile lipid accumulation in necrotic tissue. NMR Biomed 1994;7:149–155.